


Article

Band Gap and Topology of 1D Perovskite-Derived Hybrid Lead Halide Structures

Ekaterina I. Marchenko^{1,2}, Sergey A. Fateev¹, Eugene A. Goodilin^{1,3} and Alexey B. Tarasov^{1,3,*} 

¹ Laboratory of New Materials for Solar Energetics, Department of Materials Science, Lomonosov Moscow State University, 1 Lenin Hills, 119991 Moscow, Russia; marchenko-ekaterina@bk.ru (E.I.M.); saf1al@yandex.ru (S.A.F.); goodilin@yandex.ru (E.A.G.)

² Department of Geology, Lomonosov Moscow State University, 1 Lenin Hills, 119991 Moscow, Russia

³ Department of Chemistry, Lomonosov Moscow State University, 1 Lenin Hills, 119991 Moscow, Russia

* Correspondence: alexey.bor.tarasov@yandex.ru

Abstract: The unprecedented structural flexibility of hybrid halide perovskites is accompanied by a wide range of useful optoelectronic properties, causing a high interest in this family of materials. However, there are no systematic studies yet on the relationships between the topology of structures derived of chain 1D hybrid halide perovskites and their optoelectronic properties such as the band gap as already reported for 3D and 2D hybrid halide perovskites. In the present work, we introduce a rational classification of hybrid lead iodide 1D structures. We provide a theoretical assessment of the relationship between the topology of 1D hybrid halide perovskite-derived structures with vertex-connected octahedra and show that the distortions of geometry of the chains of PbI_6 octahedra are the main parameters affecting the band gap value while the distance between the chains of vertex-connected octahedra has a minor effect on the band gap.

Keywords: perovskite-derived hybrid structures; structure topology; band gap; perovskite-like; semiconductors



Citation: Marchenko, E.I.;

Fateev, S.A.; Goodilin, E.A.;

Tarasov, A.B. Band Gap and Topology of 1D Perovskite-Derived Hybrid Lead Halide Structures. *Crystals* **2022**, *12*, 657. <https://doi.org/10.3390/cryst12050657>

Academic Editor: Xiaoping Wang

Received: 28 March 2022

Accepted: 2 May 2022

Published: 4 May 2022

Publisher's Note: MDPI stays neutral with regard to jurisdictional claims in published maps and institutional affiliations.



Copyright: © 2022 by the authors. Licensee MDPI, Basel, Switzerland. This article is an open access article distributed under the terms and conditions of the Creative Commons Attribution (CC BY) license (<https://creativecommons.org/licenses/by/4.0/>).

1. Introduction

Hybrid lead halide perovskite-derived materials have been extensively studied recent years due to their potential applications in optics and optoelectronics [1,2], catalysts [3], sensors [4], and ferroelectrics [5,6]. The building blocks in the crystal structures of these materials are PbX_6 octahedra (where $\text{X} = \text{I}^-$, Br^- , Cl^-) connected along vertices, edges, or faces, that makes this family of structures to be extremely structurally diverse [7]. It is used to subdivide these materials in different groups based on the dimensionality of their inorganic sublattices: 3D, 2D, 1D and 0D [7], mainly defined by the Goldschmidt tolerance factor [8,9] and the structure of organic counterparts as shown recently [10,11]. However, hybrid halide perovskites with 3D and 2D counterparts are shown to be quite promising for photovoltaic and optoelectronic applications [1,2], the materials with 1D inorganic framework show relatively low carrier mobility and are often used as a auxiliary passivating layers to improve the device stability [12,13] rather than light absorbing/emitting materials.

The relationships between different distortions of the inorganic framework on the band gap for 3D and 2D hybrid halide perovskites have been quantitatively identified previously [14,15]; however, this question remains insufficiently explored for 1D hybrid halide structures composed of the chains of PbI_6 octahedra. Recently, Wong et al. proposed a classification system of hybrid lead halide 1D structures based on notations of PbI_6 octahedra connectivity via three main parameters: the intralayer periodicity, connectivity within the repeating unit and, finally, the connectivity to the next repeating unit [16]. At the same time, the topological description of crystal structures is becoming increasingly popular [17]. In the present work, we show that the application of alternative and more robust classification based on the topology of inorganic sublattice allows us to make

a new classification of hybrid lead halide 1D structures and to subdivide them into the subgroups for the analysis of the influence of various inorganic lattice conformations on their optoelectronic properties such as band gaps. We analyze the influence of arrangements and distortions of 1D hybrid perovskite derived structures with PbI_6 chains on their band gaps. Furthermore, we focus on the 1D perovskite-derived compounds (A_3PbI_5) exhibiting most interesting optical properties due to highly anisotropic electronic properties and highly tunable band gaps. Particularly, we analyze the influence of arrangements and distortions of vertex-connected octahedra chains on the band gaps.

2. Materials and Methods

2.1. Topological Analysis of Crystal Structures

The TOPOS program package [17,18] was used to analyze Pb-I subnets. Only the inorganic part of the structure was included in the topological analysis. The following topological parameters have been computed for all the studied experimentally refined structures from CSD database [19] (Table A1 in Appendix A). Accordingly to the terminology of nets symbols in TOPOSpro [20], the symbols of net topology ND_n , where N is a sequence of degrees (coordination numbers) of all independent nodes, D is one of the letters C , L , or T designating the dimensionality of the net (C —chain, L —layer, T —three-periodic); n enumerates non-isomorphic nets with a given ND sequence. For instance, the symbol $(2-c)3(6-c)$ denotes the chain binodal (contains two independent fragments— $(2-c)$ and $(6-c)$) net with three 2-coordinated and one 6-coordinated independent nodes (Figure 1a). The symbol $(1-c)3(2-c)(6-c)$ denotes the chain three-nodal net with four 1-coordinated, one 2-coordinated and one 6-coordinated independent nodes (Figure 1b).

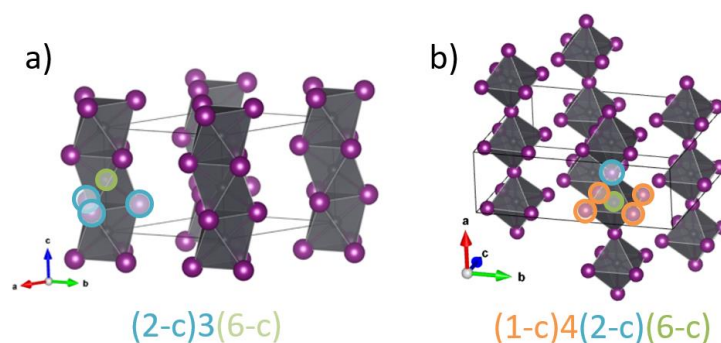


Figure 1. Scheme of net topology definition for binodal (a) and three-nodal (b) nets.

2.2. DFT Calculations

Electronic band structure calculations were obtained with the density functional theory (DFT) implemented with the Quantum ESPRESSO (version 6.1) freeware in combination with the BURAI (version 1.3.1) GUI [21–23]. The electronic exchange–correlations were treated by the Perdew–Burke–Ernzerhof (PBE) under a generalized gradient approximation (GGA) [24], and the OTFG Ultrasoft pseudo-potential was used to describe the interaction between electrons and ions [25]. Geometry optimization of the model structures was not carried out. The integration calculation of the system in Brillouin region uses the monkhorst-pack scheme, the k grid point is $2 \times 2 \times 2$ and the cut-off energy of plane wave of the system is set at 435 eV to ensure the convergence of energy and configuration of the system at the level of quasi-complete plane wave base. In the self-consistent field operation, Pulay density mixing method is adopted, and the self-consistent field is set as 5×10^{-6} eV/atom. The valence electrons involved in the calculation are $\text{Pb-}6s^26p^2$ and $\text{I-}5s^25p^5$. The calculations did not include spin–orbit coupling. A visualization of crystal structures was performed using the VESTA program [26].

2.3. Analysis of the Distortions of Structures

To identify the relationships between the distortions of the inorganic framework, the band gaps and the sizes of the A-site organic cations, we analyzed the Pearson correlation coefficients of the sizes of A-site cations with the geometric parameters of inorganic framework and calculated band gaps for the experimentally known phases with $[\text{PbI}_5]^{3-}$ chains (see Table A2). Pearson correlation coefficient is a statistical measure of the linear relationship between two variables. Pearson correlation coefficient between two variables x and y can be calculated using the following formula:

$$\frac{\sum(x_i - \bar{x})(y_i - \bar{y})}{\sqrt{\sum(x_i - \bar{x})^2 \sum(y_i - \bar{y})^2}}, \quad (1)$$

where \bar{x} is the mean value of x and \bar{y} is the mean value of y . x_i and y_i represents different values of x and y . The Pearson correlation coefficient can range from -1 to 1 .

To calculate the distortion of the inorganic framework, we used the following geometrical descriptors: the distortions of PbI_6 octahedra (Δd), distance between adjacent chains of PbI_6 octahedra (I-I distance between adjacent chains), Pb-Pb-Pb angle in a chain (Figure A2), and shortest I-I distance in a chain (Figure A2).

To determine the degree of distortion of PbI_6 octahedra, we used the equation than commonly used for evaluation of the distortion degree of perovskite-derived structures:

$$\Delta d = \frac{1}{6} \sum \left[\frac{d_n - d}{d} \right]^2, \quad (2)$$

where d_n is the individual Pb-I distances and d is the arithmetic mean values of the individual Pb-I distances.

3. Results

To reveal the topological features of 1D hybrid lead halides crystal structure, we analyzed the inorganic Pb-I subnets for 182 refined structures from the Cambridge Structural Database (CSD) [19], separated and identified nets of crystal structures and their relations using topological method that implemented in the TOPOSpro program package [17]. The structures of 1D hybrid lead halides can be distinguished in four main types according to the stoichiometry of a chain of connected octahedra and its topology notations (Figure A1, details are in Table A1 in Appendix A). The most common stoichiometry is $A(\text{PbI}_3)$ (where A is organic cations) (about 160 structures from 182) represented by two types of topology: face-connected PbI_6 octahedra formed of 2-nodal net (contains two topologically inequivalent nodes) (Figure 2a) [18] with the topology (2-c)3(6-c) and edge-connected PbI_6 octahedra with 4-nodal net topology (1-c)(2-c)(3-c)(6-c) (Figure 2b); however, there is only one experimentally refined structure with the latter chains up to now. The structures $A_4(\text{Pb}_3\text{I}_{10})$ consisting of chains of octahedra $[\text{Pb}_3\text{I}_{10}]^{4-}$ connected along edges and faces have a 5-nodal net with topology (1-c)2(2-c)2(2-c)6(6-c)2(6-c) (Figure 2c). The structures $A_2(\text{PbI}_4)$ consisting of chains of octahedra $[\text{PbI}_4]^{2-}$ connected along edges have a 3-nodal net with topology (1-c)2(2-c)2(6-c) (Figure 2d). The structures $A_3(\text{PbI}_5)$ with vertex-connected octahedra $[\text{PbI}_5]^{3-}$ chains are represented by a 3-nodal net with stoichiometry (1-c)4(2-c)(6-c) (Figure 2e).

Strictly speaking, first four types of structures are not perovskite-derived since their structures are not the derivatives of the perovskite structure type. Only the latter type of the structures with vertex-connected octahedra $[\text{PbI}_5]^{3-}$ chains preserve the fragment of perovskite structure in the form of vertex-connected 1D chains and can therefore be called a “perovskite-derived”. Such structures retain, in one of the dimensions, a high dispersion of the band characteristics of 3D halide perovskites and, accordingly, a sufficiently high mobility of charge carriers along the chains, while in the other two dimensions, a low dispersion is observed and the carriers are actually localized. Thus, the structure of 1D $A_3\text{PbI}_5$ perovskites determines the unique anisotropy of the electronic and optical

properties of these materials. The vertex connection of octahedra corresponds to the maximum number of degrees of freedom for various distortions of the 1D chain and makes it possible to vary the band gap over a wide range. Therefore, understanding of the influence of $[\text{PbI}_5]^{3-}$ chain conformations on the band gap is important for the design of new low-dimensional hybrid halide materials.

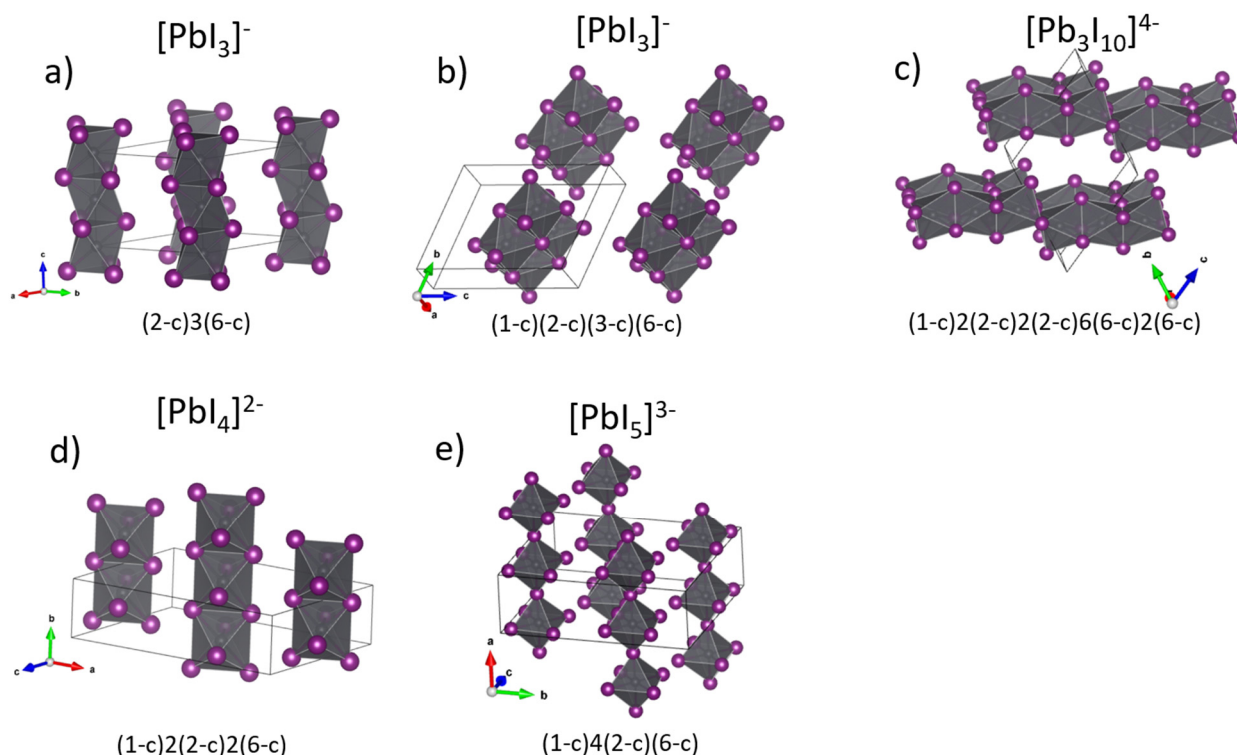


Figure 2. 1D lead-halide hybrid Pb-I subnets with different type of topology: (a,b) $[\text{PbI}_3]^-$, (c) $[\text{Pb}_3\text{I}_{10}]^{4-}$, (d) $[\text{PbI}_4]^{2-}$, (e) $[\text{PbI}_5]^{3-}$.

The relationships between the structural geometrical descriptors and the band gap for corresponding compounds with $[\text{PbI}_5]^{3-}$ chain topology were estimated using DFT calculations of the band gap of modeled structures. The following parameters were considered as relevant structural descriptors: axial and equatorial Pb–I distances, equatorial Pb–I–Pb, and tilting angles, and the distance between the $[\text{PbI}_5]^{3-}$ chains. We found that for hypothetical structures with the same Pb–I distance (3.16 Å) and without tilting of octahedra an increase in the distance between neighboring $[\text{PbI}_5]^{3-}$ chains from 4.45 Å to 7.5 Å leads to the band gap increase by 0.1 eV only (Figure 3). Thus, the geometric descriptor of the distances between the chains does not affect strongly the change in the band gap for the considered 1D structures with $[\text{PbI}_5]^{3-}$ chains since the overlap of halogen–halogen orbitals becomes insignificant at distances of 5.5 Å, similar with 2D hybrid compounds reported before [14,15,27]. It should be noted that among the experimentally known 1D hybrid halide structures with $[\text{PbI}_5]^{3-}$ chains, the minimum distance between chains is 5.14 Å (CSD ID 1048274). Thus, the main geometric factors affecting the band gap in this type of structures will be the Pb–I angles in the octahedra, the Pb–I bond lengths, and tilting of octahedra in a chain.

Figure 4 shows the calculated band structures for two hypothetical 1D perovskite-derived structures with $[\text{PbI}_5]^{3-}$ chains of vertex-connected octahedra spaced by 5.5 Å and a Pb–I bond length of 3.16 Å. The first one, featured by undistorted chains of octahedra (Figure 4a) and Pb–I–Pb angle of 180 degrees, has the band gap of 2.1 eV. In contrast, the second structure with strongly distorted chains of octahedra (Figure 4b) (the distance between the adjacent chains of 5.04 and 5.69 Å, Pb–I bond lengths in the PbI_6 octahedra

3.16 Å, 3.22 Å, 3.22 Å, 3.3 Å, 3.2 Å, 3.3 Å, the Pb-I-Pb angle between the octahedra 145 degrees) has the band gap is 2.55 eV.

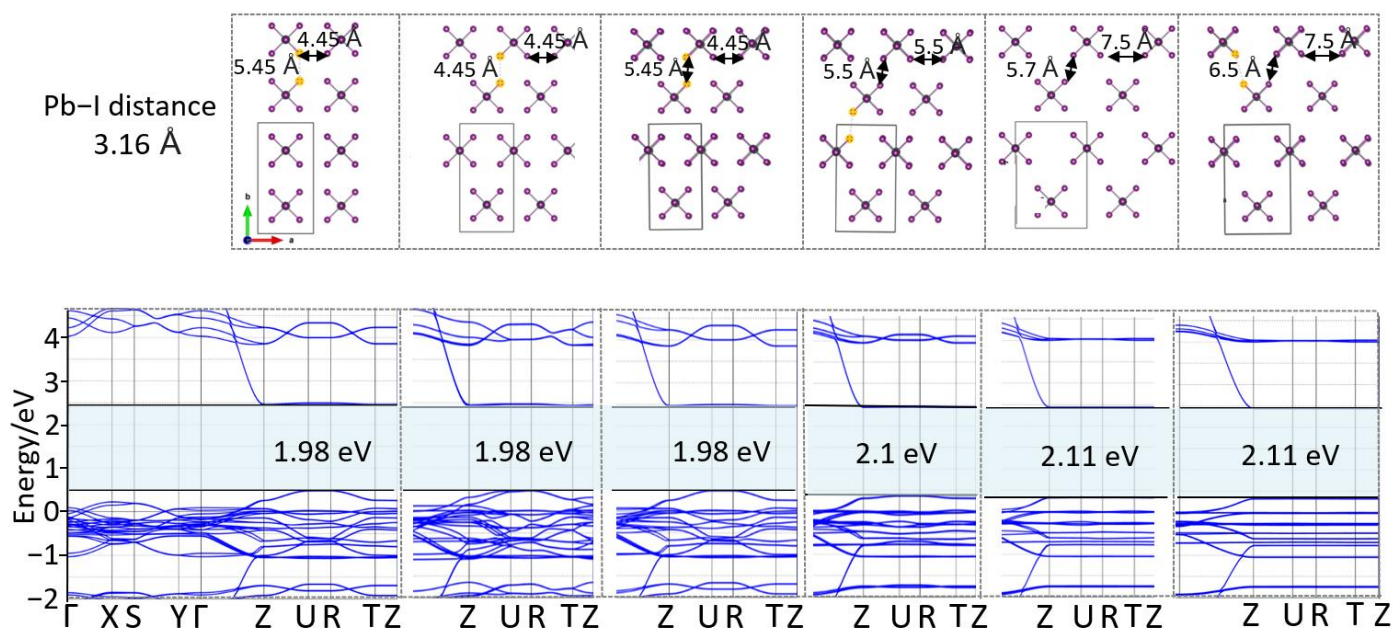


Figure 3. Calculated band structures for hypothetical 1D perovskite-derived structures with different distances between the $[\text{PbI}_5]^{3-}$ chains.

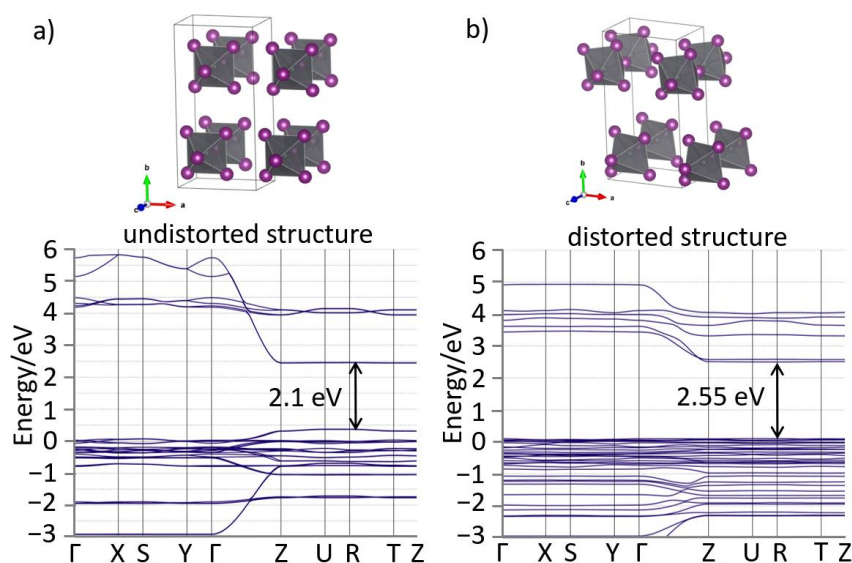


Figure 4. Calculated band structure for hypothetical undistorted (a) and distorted (b) structures of 1D perovskite-derived structures with $[\text{PbI}_5]^{3-}$ chains.

These results clearly illustrate that the distortions of geometry of the chains of PbI_6 octahedra are the main parameters affecting the band gap value, while the distance between the chains of vertex-connected octahedra has minor effect on the band gap in these materials. Therefore, while band structure of 1D hybrid halide perovskite-derived compounds is mainly defined by the size and geometry of organic cations, occupying the interchain space, the band gap of such compounds can be tuned in range from 1.98 eV to 2.55 eV by choosing an appropriate organic counterpart.

To confirm our conclusions, we considered the experimental crystal structures of perovskite-derived compounds with vertex-connected octahedra $[\text{PbI}_5]^{3-}$ chains (see

Table A1). For these compounds we calculated the band gap values, values of organic cations and geometric parameters of the distortion of the structures (Table A2): the distortion of the Pb-I bond length in PbI_6 octahedra (Δd), the distance between adjacent chains of vertex-connected octahedra, Pb-Pb-Pb angles in a chain (see Figure A2), and shortest I-I distance in a chain (see Figure A2). The heatmap of Pearson correlation coefficients clearly illustrates that the descriptors of shortest I-I distance in a chain of octahedra and Pb-Pb-Pb angle in a chain (Figure A2) are responsible for rotations and tilts of octahedra in chains relative to each other. Interestingly, that the Pearson correlation coefficient between shortest I-I distance in a chain of octahedra (Figure A2) and Δd is strongly negative (-0.95), while the correlation coefficient between shortest I-I distance in a chain of octahedra and Pb-Pb-Pb angle in a chain is positive (0.72). Thus, the distortions of octahedra chains affect the Pb-I distance in the octahedra (Δd), and hence the band gap. The Pearson correlation coefficient between the Δd and the band gap is strongly positive (0.82) for the considered experimental compounds. To summarize, an increase of the distortions of the Pb-I distances in octahedra (Δd) lead to an increase in the band gap, and a decrease in the shortest I-I distances in octahedra chains also leads to an increase in the Δd and to an increase in a chain tilting. It is worth noting that for the experimentally known 1D perovskite-derived structures with vertex-connected chains of PbI_6 octahedra and various organic cations, the Pearson correlations of the “A-site” cation sizes with the band gap and geometrical distortions in octahedra are weakly positive (0.5 and 0.46 , respectively) (Figure 5).

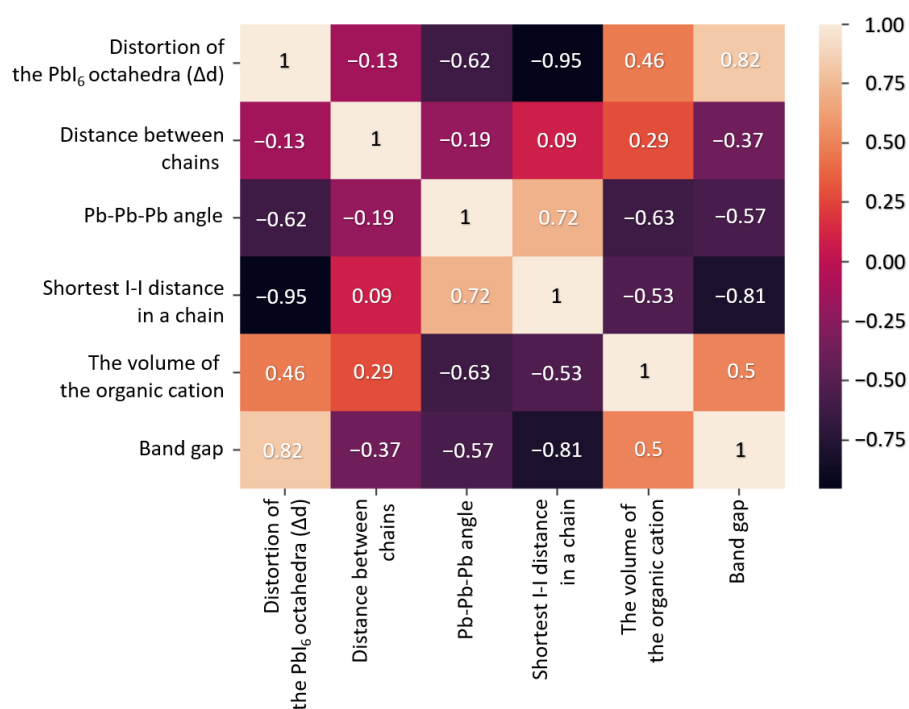


Figure 5. Heatmap of Pearson correlation coefficient matrix for geometrical descriptors and the band gaps of 1D perovskite-derived experimental structures with vertex-connected chains of PbI_6 octahedra.

4. Conclusions

To summarize, we introduce a topological classification of 1D hybrid lead halide structures with chains of lead halide octahedra revealing five different types of such structures. We estimated an influence of the distortions in inorganic frameworks of 1D hybrid halide perovskite-derived structures with vertex-connected octahedra and $[\text{PbI}_5]^{3-}$ stoichiometry on their band gaps. It was shown that the distortions of geometry of the chains of PbI_6 octahedra are the main parameters affecting the band gap value and turning them in range from 2.10 eV to 2.55 eV, whereas a shortening of the distance (d) leads to

a decrease in the band gap to 1.98 eV, and in the case of d greater than 5.5 Å, it actually does not affect the E_g .

Author Contributions: Conceptualization, E.I.M., S.A.F. and A.B.T.; methodology, E.I.M.; writing—original draft preparation, E.I.M., S.A.F., A.B.T. and E.A.G.; supervision, E.A.G. and A.B.T. All authors have read and agreed to the published version of the manuscript.

Funding: This work was financially supported by a grant from the Russian Science Foundation, Project No. 19-73-30022.

Data Availability Statement: Data available on request.

Conflicts of Interest: The authors declare that they have no conflict of interest.

Appendix A

Table A1. Net topology of 1D hybrid lead halide structures from CSD database using TOPOSpro program package.

CSD Ref Code	Type of Chain	Topology of the Net *
214790	chains [0 1 0] with $[\text{Pb}_3\text{I}_{10}]^{4-}$	1,2,2,6,6-c net with stoichiometry (1-c)2(2-c)6(2-c)2(6-c)(6-c)2; 5-nodal net
104219	chains [1 0 1] with $[\text{Pb}_3\text{I}_{10}]^{4-}$	1,2,2,6,6-c net with stoichiometry (1-c)2(2-c)6(2-c)2(6-c)(6-c)2; 5-nodal net
82074	chains [0 0 1] with $[\text{Pb}_3\text{I}_{10}]^{4-}$	1,2,2,6,6-c net with stoichiometry (1-c)2(2-c)2(2-c)6(6-c)2(6-c); 5-nodal net
836347	chains [0 1 -1] with $[\text{Pb}_3\text{I}_{10}]^{4-}$	1,2,2,6,6-c net with stoichiometry (1-c)2(2-c)2(2-c)6(6-c)2(6-c); 5-nodal net
1119690	chains [1 0 0] with $[\text{Pb}_3\text{I}_{10}]^{4-}$	1,2,2,6,6-c net with stoichiometry (1-c)2(2-c)2(2-c)6(6-c)2(6-c); 5-nodal net
1515524-957318	chains [1 0 1] with $[\text{Pb}_3\text{I}_{10}]^{4-}$	1,2,2,6,6-c net with stoichiometry (1-c)2(2-c)2(2-c)6(6-c)2(6-c); 5-nodal net
1515524-957318	chains [1 0 1] with $[\text{Pb}_3\text{I}_{10}]^{4-}$	1,2,2,6,6-c net with stoichiometry (1-c)2(2-c)2(2-c)6(6-c)2(6-c); 5-nodal net
1945576	chains [1 0 1] with $[\text{Pb}_3\text{I}_{10}]^{4-}$	1,2,2,6,6-c net with stoichiometry (1-c)2(2-c)2(2-c)6(6-c)2(6-c); 5-nodal net
160842	chains [0 0 1] with $[\text{PbI}_3]^-$	2,6-c net with stoichiometry (2-c)3(6-c); 2-nodal net
210812	chains [0 0 1] with $[\text{PbI}_3]^-$	2,6-c net with stoichiometry (2-c)3(6-c); 2-nodal net
254879	chains [0 0 1] with $[\text{PbI}_3]^-$	2,6-c net with stoichiometry (2-c)3(6-c); 2-nodal net
277224	chains [0 0 1] with $[\text{PbI}_3]^-$	2,6-c net with stoichiometry (2-c)3(6-c); 2-nodal net
790923	chains [0 0 1] with $[\text{PbI}_3]^-$	2,6-c net with stoichiometry (2-c)3(6-c); 2-nodal net
291886	chains [0 0 1] with $[\text{PbI}_3]^-$	2,6-c net with stoichiometry (2-c)3(6-c); 2-nodal net
298933	chains [0 0 1] with $[\text{PbI}_3]^-$	2,6-c net with stoichiometry (2-c)3(6-c); 2-nodal net
604996	chains [0 0 1] with $[\text{PbI}_3]^-$	2,6-c net with stoichiometry (2-c)3(6-c); 2-nodal net
609997	chains [0 0 1] with $[\text{PbI}_3]^-$	2,6-c net with stoichiometry (2-c)3(6-c); 2-nodal net
632026	chains [0 0 1] with $[\text{PbI}_3]^-$	2,6-c net with stoichiometry (2-c)3(6-c); 2-nodal net
636241	chains [0 0 1] with $[\text{PbI}_3]^-$	2,6-c net with stoichiometry (2-c)3(6-c); 2-nodal net
722539	chains [0 0 1] with $[\text{PbI}_3]^-$	2,6-c net with stoichiometry (2-c)3(6-c); 2-nodal net
776897	chains [0 0 1] with $[\text{PbI}_3]^-$	2,6-c net with stoichiometry (2-c)3(6-c); 2-nodal net
780403	chains [0 0 1] with $[\text{PbI}_3]^-$	2,6-c net with stoichiometry (2-c)3(6-c); 2-nodal net
780404	chains [0 0 1] with $[\text{PbI}_3]^-$	2,6-c net with stoichiometry (2-c)3(6-c); 2-nodal net
780405	chains [0 0 1] with $[\text{PbI}_3]^-$	2,6-c net with stoichiometry (2-c)3(6-c); 2-nodal net
780408	chains [0 0 1] with $[\text{PbI}_3]^-$	2,6-c net with stoichiometry (2-c)3(6-c); 2-nodal net
780409	chains [0 0 1] with $[\text{PbI}_3]^-$	2,6-c net with stoichiometry (2-c)3(6-c); 2-nodal net
921641	chains [0 0 1] with $[\text{PbI}_3]^-$	2,6-c net with stoichiometry (2-c)3(6-c); 2-nodal net
780410	chains [0 0 1] with $[\text{PbI}_3]^-$	2,6-c net with stoichiometry (2-c)3(6-c); 2-nodal net

Table A1. Cont.

CSD Ref Code	Type of Chain	Topology of the Net *
785767	chains [0 0 1] with [PbI ₃] [−]	2,6-c net with stoichiometry (2-c)3(6-c); 2-nodal net
785768	chains [0 0 1] with [PbI ₃] [−]	2,6-c net with stoichiometry (2-c)3(6-c); 2-nodal net
785769	chains [0 0 1] with [PbI ₃] [−]	2,6-c net with stoichiometry (2-c)3(6-c); 2-nodal net
818548	chains [0 0 1] with [PbI ₃] [−]	2,6-c net with stoichiometry (2-c)3(6-c); 2-nodal net
834146	chains [0 0 1] with [PbI ₃] [−]	2,6-c net with stoichiometry (2-c)3(6-c); 2-nodal net
836348	chains [0 0 1] with [PbI ₃] [−]	2,6-c net with stoichiometry (2-c)3(6-c); 2-nodal net
917236	chains [0 0 1] with [PbI ₃] [−]	2,6-c net with stoichiometry (2-c)3(6-c); 2-nodal net
1012805	chains [0 0 1] with [PbI ₃] [−]	2,6-c net with stoichiometry (2-c)3(6-c); 2-nodal net
1123333	chains [0 0 1] with [PbI ₃] [−]	2,6-c net with stoichiometry (2-c)3(6-c); 2-nodal net
1869662	chains [0 0 1] with [PbI ₃] [−]	2,6-c net with stoichiometry (2-c)3(6-c); 2-nodal net
1869662	chains [0 0 1] with [PbI ₃] [−]	2,6-c net with stoichiometry (2-c)3(6-c); 2-nodal net
1869663	chains [0 0 1] with [PbI ₃] [−]	2,6-c net with stoichiometry (2-c)3(6-c); 2-nodal net
1135285	chains [0 0 1] with [PbI ₃] [−]	2,6-c net with stoichiometry (2-c)3(6-c); 2-nodal net
1962916	chains [0 0 1] with [PbI ₃] [−]	2,6-c net with stoichiometry (2-c)3(6-c); 2-nodal net
1183349	chains [0 0 1] with [PbI ₃] [−]	2,6-c net with stoichiometry (2-c)3(6-c); 2-nodal net
1308385	chains [0 0 1] with [PbI ₃] [−]	2,6-c net with stoichiometry (2-c)3(6-c); 2-nodal net
1400319	chains [0 0 1] with [PbI ₃] [−]	2,6-c net with stoichiometry (2-c)3(6-c); 2-nodal net
1400321	chains [0 0 1] with [PbI ₃] [−]	2,6-c net with stoichiometry (2-c)3(6-c); 2-nodal net
1400323	chains [0 0 1] with [PbI ₃] [−]	2,6-c net with stoichiometry (2-c)3(6-c); 2-nodal net
1400324-15701131	chains [0 0 1] with [PbI ₃] [−]	2,6-c net with stoichiometry (2-c)3(6-c); 2-nodal net
1400324-15701131	chains [0 0 1] with [PbI ₃] [−]	2,6-c net with stoichiometry (2-c)3(6-c); 2-nodal net
1400324-15701131	chains [0 0 1] with [PbI ₃] [−]	2,6-c net with stoichiometry (2-c)3(6-c); 2-nodal net
1400324-15701131	chains [0 0 1] with [PbI ₃] [−]	2,6-c net with stoichiometry (2-c)3(6-c); 2-nodal net
1400324-15701131	chains [0 0 1] with [PbI ₃] [−]	2,6-c net with stoichiometry (2-c)3(6-c); 2-nodal net
1432458-1822500	chains [0 0 1] with [PbI ₃] [−]	2,6-c net with stoichiometry (2-c)3(6-c); 2-nodal net
1432458-1822500	chains [0 0 1] with [PbI ₃] [−]	2,6-c net with stoichiometry (2-c)3(6-c); 2-nodal net
1495871	chains [0 0 1] with [PbI ₃] [−]	2,6-c net with stoichiometry (2-c)3(6-c); 2-nodal net
1526831	chains [0 0 1] with [PbI ₃] [−]	2,6-c net with stoichiometry (2-c)3(6-c); 2-nodal net
1532918-968126	chains [0 0 1] with [PbI ₃] [−]	2,6-c net with stoichiometry (2-c)3(6-c); 2-nodal net
1547867	chains [0 0 1] with [PbI ₃] [−]	2,6-c net with stoichiometry (2-c)3(6-c); 2-nodal net
1570129	chains [0 0 1] with [PbI ₃] [−]	2,6-c net with stoichiometry (2-c)3(6-c); 2-nodal net
1590157-1858276	chains [0 0 1] with [PbI ₃] [−]	2,6-c net with stoichiometry (2-c)3(6-c); 2-nodal net
1590177	chains [0 0 1] with [PbI ₃] [−]	2,6-c net with stoichiometry (2-c)3(6-c); 2-nodal net
1819979	chains [0 0 1] with [PbI ₃] [−]	2,6-c net with stoichiometry (2-c)3(6-c); 2-nodal net
1828821	chains [0 0 1] with [PbI ₃] [−]	2,6-c net with stoichiometry (2-c)3(6-c); 2-nodal net
1828823	chains [0 0 1] with [PbI ₃] [−]	2,6-c net with stoichiometry (2-c)3(6-c); 2-nodal net
1853250	chains [0 0 1] with [PbI ₃] [−]	2,6-c net with stoichiometry (2-c)3(6-c); 2-nodal net
1869657-1869658	chains [0 0 1] with [PbI ₃] [−]	2,6-c net with stoichiometry (2-c)3(6-c); 2-nodal net
1869657-1869658	chains [0 0 1] with [PbI ₃] [−]	2,6-c net with stoichiometry (2-c)3(6-c); 2-nodal net
1869657-1869658	chains [0 0 1] with [PbI ₃] [−]	2,6-c net with stoichiometry (2-c)3(6-c); 2-nodal net
1905762	chains [0 0 1] with [PbI ₃] [−]	2,6-c net with stoichiometry (2-c)3(6-c); 2-nodal net

Table A1. Cont.

CSD Ref Code	Type of Chain	Topology of the Net *
1909463	chains [0 0 1] with [PbI ₃] [−]	2,6-c net with stoichiometry (2-c)3(6-c); 2-nodal net
1923364-1923365	chains [0 0 1] with [PbI ₃] [−]	2,6-c net with stoichiometry (2-c)3(6-c); 2-nodal net
1934893-1934898	chains [0 0 1] with [PbI ₃] [−]	2,6-c net with stoichiometry (2-c)3(6-c); 2-nodal net
1934893-1934898	chains [0 0 1] with [PbI ₃] [−]	2,6-c net with stoichiometry (2-c)3(6-c); 2-nodal net
1934900	chains [0 0 1] with [PbI ₃] [−]	2,6-c net with stoichiometry (2-c)3(6-c); 2-nodal net
1944788	chains [0 0 1] with [PbI ₃] [−]	2,6-c net with stoichiometry (2-c)3(6-c); 2-nodal net
1969340	chains [0 0 1] with [PbI ₃] [−]	2,6-c net with stoichiometry (2-c)3(6-c); 2-nodal net
1992695	chains [0 0 1] with [PbI ₃] [−]	2,6-c net with stoichiometry (2-c)3(6-c); 2-nodal net
1992696	chains [0 0 1] with [PbI ₃] [−]	2,6-c net with stoichiometry (2-c)3(6-c); 2-nodal net
2072691-994664	chains [0 0 1] with [PbI ₃] [−]	2,6-c net with stoichiometry (2-c)3(6-c); 2-nodal net
2072691-994664	chains [0 0 1] with [PbI ₃] [−]	2,6-c net with stoichiometry (2-c)3(6-c); 2-nodal net
2072691-994664	chains [0 0 1] with [PbI ₃] [−]	2,6-c net with stoichiometry (2-c)3(6-c); 2-nodal net
2072691-994664	chains [0 0 1] with [PbI ₃] [−]	2,6-c net with stoichiometry (2-c)3(6-c); 2-nodal net
2072691-994664	chains [0 0 1] with [PbI ₃] [−]	2,6-c net with stoichiometry (2-c)3(6-c); 2-nodal net
219758.cif.	chains [0 0 1] with [PbI ₃] [−]	2,6-c net with stoichiometry (2-c)3(6-c); 2-nodal net
708406	chains [0 1 0] with [PbI ₃] [−]	2,6-c net with stoichiometry (2-c)3(6-c); 2-nodal net
780407	chains [0 1 0] with [PbI ₃] [−]	2,6-c net with stoichiometry (2-c)3(6-c); 2-nodal net
797634	chains [0 1 0] with [PbI ₃] [−]	2,6-c net with stoichiometry (2-c)3(6-c); 2-nodal net
861679	chains [0 1 0] with [PbI ₃] [−]	2,6-c net with stoichiometry (2-c)3(6-c); 2-nodal net
1048276	chains [0 1 0] with [PbI ₃] [−]	2,6-c net with stoichiometry (2-c)3(6-c); 2-nodal net
1135285-1962916	chains [0 1 0] with [PbI ₃] [−]	2,6-c net with stoichiometry (2-c)3(6-c); 2-nodal net
1169102	chains [0 1 0] with [PbI ₃] [−]	2,6-c net with stoichiometry (2-c)3(6-c); 2-nodal net
1871034	chains [0 1 0] with [PbI ₃] [−]	2,6-c net with stoichiometry (2-c)3(6-c); 2-nodal net
1400322	chains [0 1 0] with [PbI ₃] [−]	2,6-c net with stoichiometry (2-c)3(6-c); 2-nodal net
1495872	chains [0 1 0] with [PbI ₃] [−]	2,6-c net with stoichiometry (2-c)3(6-c); 2-nodal net
1495874	chains [0 1 0] with [PbI ₃] [−]	2,6-c net with stoichiometry (2-c)3(6-c); 2-nodal net
1502217	chains [0 1 0] with [PbI ₃] [−]	2,6-c net with stoichiometry (2-c)3(6-c); 2-nodal net
1504241	chains [0 1 0] with [PbI ₃] [−]	2,6-c net with stoichiometry (2-c)3(6-c); 2-nodal net
1524688-1944787	chains [0 1 0] with [PbI ₃] [−]	2,6-c net with stoichiometry (2-c)3(6-c); 2-nodal net
1524688-1944787	chains [0 1 0] with [PbI ₃] [−]	2,6-c net with stoichiometry (2-c)3(6-c); 2-nodal net
1524689	chains [0 1 0] with [PbI ₃] [−]	2,6-c net with stoichiometry (2-c)3(6-c); 2-nodal net
1562186	chains [0 1 0] with [PbI ₃] [−]	2,6-c net with stoichiometry (2-c)3(6-c); 2-nodal net
1577162-1577163	chains [0 1 0] with [PbI ₃] [−]	2,6-c net with stoichiometry (2-c)3(6-c); 2-nodal net
1828819	chains [0 1 0] with [PbI ₃] [−]	2,6-c net with stoichiometry (2-c)3(6-c); 2-nodal net
1871034	chains [0 1 0] with [PbI ₃] [−]	2,6-c net with stoichiometry (2-c)3(6-c); 2-nodal net
1901048-612444	chains [0 1 0] with [PbI ₃] [−]	2,6-c net with stoichiometry (2-c)3(6-c); 2-nodal net
1901048-612444	chains [0 1 0] with [PbI ₃] [−]	2,6-c net with stoichiometry (2-c)3(6-c); 2-nodal net
1915775	chains [0 1 0] with [PbI ₃] [−]	2,6-c net with stoichiometry (2-c)3(6-c); 2-nodal net
1923364-1923365	chains [0 1 0] with [PbI ₃] [−]	2,6-c net with stoichiometry (2-c)3(6-c); 2-nodal net
1944787	chains [0 1 0] with [PbI ₃] [−]	2,6-c net with stoichiometry (2-c)3(6-c); 2-nodal net
1962916	chains [0 1 0] with [PbI ₃] [−]	2,6-c net with stoichiometry (2-c)3(6-c); 2-nodal net

Table A1. Cont.

CSD Ref Code	Type of Chain	Topology of the Net *
1977726	chains [0 1 0] with [PbI ₃] [−]	2,6-c net with stoichiometry (2-c)3(6-c); 2-nodal net
1024096	chains [0 1 −1] with [PbI ₃] [−]	2,6-c net with stoichiometry (2-c)3(6-c); 2-nodal net
221315	chains [1 0 0] with [PbI ₃] [−]	2,6-c net with stoichiometry (2-c)3(6-c); 2-nodal net
248812	chains [1 0 0] with [PbI ₃] [−]	2,6-c net with stoichiometry (2-c)3(6-c); 2-nodal net
776896	chains [1 0 0] with [PbI ₃] [−]	2,6-c net with stoichiometry (2-c)3(6-c); 2-nodal net
776898	chains [1 0 0] with [PbI ₃] [−]	2,6-c net with stoichiometry (2-c)3(6-c); 2-nodal net
776899	chains [1 0 0] with [PbI ₃] [−]	2,6-c net with stoichiometry (2-c)3(6-c); 2-nodal net
900606	chains [1 0 0] with [PbI ₃] [−]	2,6-c net with stoichiometry (2-c)3(6-c); 2-nodal net
958061	chains [1 0 0] with [PbI ₃] [−]	2,6-c net with stoichiometry (2-c)3(6-c); 2-nodal net
967300	chains [1 0 0] with [PbI ₃] [−]	2,6-c net with stoichiometry (2-c)3(6-c); 2-nodal net
998856	chains [1 0 0] with [PbI ₃] [−]	2,6-c net with stoichiometry (2-c)3(6-c); 2-nodal net
1015245	chains [1 0 0] with [PbI ₃] [−]	2,6-c net with stoichiometry (2-c)3(6-c); 2-nodal net
1047834	chains [1 0 0] with [PbI ₃] [−]	2,6-c net with stoichiometry (2-c)3(6-c); 2-nodal net
1251540	chains [1 0 0] with [PbI ₃] [−]	2,6-c net with stoichiometry (2-c)3(6-c); 2-nodal net
1274099	chains [1 0 0] with [PbI ₃] [−]	2,6-c net with stoichiometry (2-c)3(6-c); 2-nodal net
1447264	chains [1 0 0] with [PbI ₃] [−]	2,6-c net with stoichiometry (2-c)3(6-c); 2-nodal net
1447265	chains [1 0 0] with [PbI ₃] [−]	2,6-c net with stoichiometry (2-c)3(6-c); 2-nodal net
1447266	chains [1 0 0] with [PbI ₃] [−]	2,6-c net with stoichiometry (2-c)3(6-c); 2-nodal net
1483105-871217	chains [1 0 0] with [PbI ₃] [−]	2,6-c net with stoichiometry (2-c)3(6-c); 2-nodal net
1483105-871217	chains [1 0 0] with [PbI ₃] [−]	2,6-c net with stoichiometry (2-c)3(6-c); 2-nodal net
1495875	chains [1 0 0] with [PbI ₃] [−]	2,6-c net with stoichiometry (2-c)3(6-c); 2-nodal net
1523553-1523557	chains [1 0 0] with [PbI ₃] [−]	2,6-c net with stoichiometry (2-c)3(6-c); 2-nodal net
1523553-1523557	chains [1 0 0] with [PbI ₃] [−]	2,6-c net with stoichiometry (2-c)3(6-c); 2-nodal net
1523553-1523557	chains [1 0 0] with [PbI ₃] [−]	2,6-c net with stoichiometry (2-c)3(6-c); 2-nodal net
1523553-1523557	chains [1 0 0] with [PbI ₃] [−]	2,6-c net with stoichiometry (2-c)3(6-c); 2-nodal net
1533556	chains [1 0 0] with [PbI ₃] [−]	2,6-c net with stoichiometry (2-c)3(6-c); 2-nodal net
1535129-1535132	chains [1 0 0] with [PbI ₃] [−]	2,6-c net with stoichiometry (2-c)3(6-c); 2-nodal net
1535129-1535132	chains [1 0 0] with [PbI ₃] [−]	2,6-c net with stoichiometry (2-c)3(6-c); 2-nodal net
1535129-1535132	chains [1 0 0] with [PbI ₃] [−]	2,6-c net with stoichiometry (2-c)3(6-c); 2-nodal net
1535129-1535132	chains [1 0 0] with [PbI ₃] [−]	2,6-c net with stoichiometry (2-c)3(6-c); 2-nodal net
1577162-1577163	chains [1 0 0] with [PbI ₃] [−]	2,6-c net with stoichiometry (2-c)3(6-c); 2-nodal net
1590186	chains [1 0 0] with [PbI ₃] [−]	2,6-c net with stoichiometry (2-c)3(6-c); 2-nodal net
1828826	chains [1 0 0] with [PbI ₃] [−]	2,6-c net with stoichiometry (2-c)3(6-c); 2-nodal net
1846735	chains [1 0 0] with [PbI ₃] [−]	2,6-c net with stoichiometry (2-c)3(6-c); 2-nodal net
1874395	chains [1 0 0] with [PbI ₃] [−]	2,6-c net with stoichiometry (2-c)3(6-c); 2-nodal net
1877051	chains [1 0 0] with [PbI ₃] [−]	2,6-c net with stoichiometry (2-c)3(6-c); 2-nodal net
1877051-607736	chains [1 0 0] with [PbI ₃] [−]	2,6-c net with stoichiometry (2-c)3(6-c); 2-nodal net
1877051-607736	chains [1 0 0] with [PbI ₃] [−]	2,6-c net with stoichiometry (2-c)3(6-c); 2-nodal net
1877055-607737	chains [1 0 0] with [PbI ₃] [−]	2,6-c net with stoichiometry (2-c)3(6-c); 2-nodal net
1877055-607737	chains [1 0 0] with [PbI ₃] [−]	2,6-c net with stoichiometry (2-c)3(6-c); 2-nodal net
1899647	chains [1 0 0] with [PbI ₃] [−]	2,6-c net with stoichiometry (2-c)3(6-c); 2-nodal net

Table A1. Cont.

CSD Ref Code	Type of Chain	Topology of the Net *
1902819	chains [1 0 0] with [PbI ₃] [−]	2,6-c net with stoichiometry (2-c)3(6-c); 2-nodal net
1934897-1934902	chains [1 0 0] with [PbI ₃] [−]	2,6-c net with stoichiometry (2-c)3(6-c); 2-nodal net
1934897-1934902	chains [1 0 0] with [PbI ₃] [−]	2,6-c net with stoichiometry (2-c)3(6-c); 2-nodal net
1934902	chains [1 0 0] with [PbI ₃] [−]	2,6-c net with stoichiometry (2-c)3(6-c); 2-nodal net
1944781	chains [1 0 0] with [PbI ₃] [−]	2,6-c net with stoichiometry (2-c)3(6-c); 2-nodal net
1944784	chains [1 0 0] with [PbI ₃] [−]	2,6-c net with stoichiometry (2-c)3(6-c); 2-nodal net
1944785	chains [1 0 0] with [PbI ₃] [−]	2,6-c net with stoichiometry (2-c)3(6-c); 2-nodal net
776895	chains [1 0 1] with [PbI ₃] [−]	2,6-c net with stoichiometry (2-c)3(6-c); 2-nodal net
1483104	chains [1 0 1] with [PbI ₃] [−]	2,6-c net with stoichiometry (2-c)3(6-c); 2-nodal net
1869657-1869658	chains [1 0 1] with [PbI ₃] [−]	2,6-c net with stoichiometry (2-c)3(6-c); 2-nodal net
1869657-1869658	chains [1 0 1] with [PbI ₃] [−]	2,6-c net with stoichiometry (2-c)3(6-c); 2-nodal net
114129	chains [1 1 1] with [PbI ₃] [−]	2,6-c net with stoichiometry (2-c)3(6-c); 2-nodal net
734814	chains [1 1 1] with [PbI ₃] [−]	2,6-c net with stoichiometry (2-c)3(6-c); 2-nodal net
735413	chains [1 1 1] with [PbI ₃] [−]	2,6-c net with stoichiometry (2-c)3(6-c); 2-nodal net
745950	chains [1 1 1] with [PbI ₃] [−]	2,6-c net with stoichiometry (2-c)3(6-c); 2-nodal net
1400320	chains [1 0 0] with [PbI ₃] [−]	1,2,3,6-c net with stoichiometry (1-c)(2-c)(3-c)(6-c); 4-nodal net
1894399	chains [1 0 0] with [PbI ₃] [−]	1,2,3,6-c net with stoichiometry (1-c)(2-c)(3-c)(6-c); 4-nodal net
1968137	chains [0 0 1] with [PbI ₄] ^{2−}	1,2,6-c net with stoichiometry (1-c)2(2-c)2(6-c); 3-nodal net
1432454	chains [1 0 0] with [PbI ₄] ^{2−}	1,2,6-c net with stoichiometry (1-c)2(2-c)2(6-c); 3-nodal net
1846083	chains [0 1 0] with [PbI ₄] ^{2−}	1,2,6-c net with stoichiometry (1-c)2(2-c)2(6-c); 3-nodal net
1938185	chains [0 0 1] with [PbI ₄] ^{2−}	1,2,6-c net with stoichiometry (1-c)2(2-c)2(6-c); 3-nodal net
1307516	chains [0 0 1] with [PbI ₅] ^{3−}	1,2,6-c net with stoichiometry (1-c)4(2-c)(6-c); 3-nodal net
1429047	chains [0 0 1] with [PbI ₅] ^{3−}	1,2,6-c net with stoichiometry (1-c)4(2-c)(6-c); 3-nodal net
1910573	chains [0 0 1] with [PbI ₅] ^{3−}	1,2,6-c net with stoichiometry (1-c)4(2-c)(6-c); 3-nodal net
1860735-1861695	chains [0 0 1] with [PbI ₅] ^{3−}	1,2,6-c net with stoichiometry (1-c)4(2-c)(6-c); 3-nodal net
1860735-1861695	chains [0 0 1] with [PbI ₅] ^{3−}	1,2,6-c net with stoichiometry (1-c)4(2-c)(6-c); 3-nodal net
1860735-1861695	chains [0 0 1] with [PbI ₅] ^{3−}	1,2,6-c net with stoichiometry (1-c)4(2-c)(6-c); 3-nodal net
1860735-1861695	chains [0 0 1] with [PbI ₅] ^{3−}	1,2,6-c net with stoichiometry (1-c)4(2-c)(6-c); 3-nodal net
1048274	chains [0 1 0] with [PbI ₅] ^{3−}	1,2,6-c net with stoichiometry (1-c)4(2-c)(6-c); 3-nodal net
1505390	chains [0 1 0] with [PbI ₅] ^{3−}	1,2,6-c net with stoichiometry (1-c)4(2-c)(6-c); 3-nodal net

* Network stoichiometry means the number of different independent nodes in the net.

Table A2. The geometrical distortions and calculated band gaps for hybrid perovskite-derived structures with [PbI₅]^{3−} vertex-connected chains.

Reference	Organic Cation	Distortion of Octahedra (Δd)	Distance between Chains, Å	Pb-Pb-Pb Angle, °	Shortest I-I Distance in a Chain of Octahedra, Å	The Volume of the Organic Cation in the Structure, Å ³	Calculated Band Gap, eV
[28]	piperazine-1,4-dium	7.27×10^{-4}	7.08	83.127	4.16	179.94	2.15
[29]	methylammonium, DMSO	5.72×10^{-4}	4.334	173.73	4.614	120.36	2.26
[30]	guanidinium	2.48×10^{-5}	6.65	180	6.36	112.99	2.01

Table A2. Cont.

Reference	Organic Cation	Distortion of Octahedra (Δd)	Distance between Chains, Å	Pb-Pb-Pb Angle, °	Shortest I-I Distance in a Chain of Octahedra, Å	The Volume of the Organic Cation in the Structure, Å ³	Calculated Band Gap, eV
[30]	guanidinium	7.39×10^{-5}	6.9	180	6.44	93.39	2.04
[30]	guanidinium	2.53×10^{-5}	6.65	180	6.36	123.6	2.01
[30]	guanidinium	5.17×10^{-5}	4.914	180	6.48	142.14	1.99
[31]	iso-propylammonium	3.35×10^{-4}	4.7	89.75	5.06	115.53	2.25
[32]	iodoformamidinium	2.62×10^{-4}	5.167	180	6.42	104.49	2.18
[33]	tetraethylenepentamine	5.94×10^{-4}	6.538	84.53	4.25	399.43	2.33

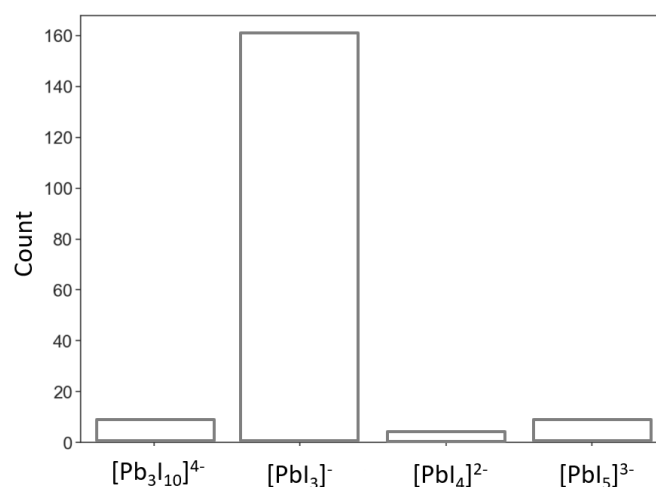


Figure A1. The distribution of the 1D Pb-I experimentally refined structures from ICSD by point symbol for net.

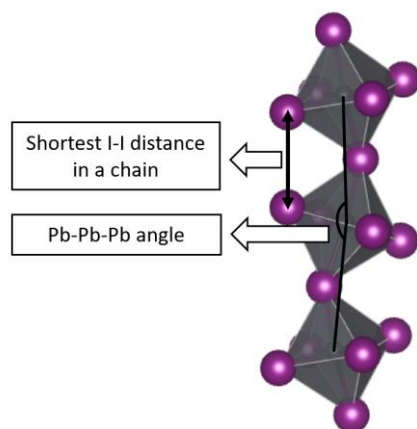


Figure A2. Geometrical descriptors used for analysis of the distortions of inorganic framework.

References

- Wang, G.E.; Xu, G.; Wang, M.S.; Cai, L.Z.; Li, W.H.; Guo, G.C. Semiconductive 3-D haloplumbate framework hybrids with high color rendering index white-light emission. *Chem. Sci.* **2015**, *6*, 7222–7226. [[CrossRef](#)] [[PubMed](#)]
- Wang, G.E.; Jiang, X.M.; Zhang, M.J.; Chen, H.F.; Liu, B.W.; Wang, M.S.; Guo, G.C. Crystal structures and optical properties of iodoplumbates hybrids templated by in situ synthesized 1,4-diazabicyclo [2.2.2]octane derivatives. *CrystEngComm* **2013**, *15*, 10399–10404. [[CrossRef](#)]
- Liu, G.N.; Zhao, R.Y.; Xu, B.; Sun, Y.; Jiang, X.M.; Hu, X.; Li, C. Design, Synthesis, and Photocatalytic Application of Moisture-Stable Hybrid Lead-Free Perovskite. *ACS Appl. Mater. Interfaces* **2020**, *12*, 54694–54702. [[CrossRef](#)] [[PubMed](#)]
- Harwell, J.R.; Glackin, J.M.E.; Davis, N.J.L.K.; Gillanders, R.N.; Credgington, D.; Turnbull, G.A.; Samuel, I.D.W. Sensing of explosive vapor by hybrid perovskites: Effect of dimensionality. *APL Mater.* **2020**, *8*, 071106. [[CrossRef](#)]

5. Chen, X.G.; Song, X.J.; Zhang, Z.X.; Zhang, H.Y.; Pan, Q.; Yao, J.; You, Y.M.; Xiong, R.G. Confinement-Driven Ferroelectricity in a Two-Dimensional Hybrid Lead Iodide Perovskite. *J. Am. Chem. Soc.* **2020**, *142*, 10212–10218. [[CrossRef](#)] [[PubMed](#)]
6. Zhang, H.Y.; Song, X.J.; Cheng, H.; Zeng, Y.L.; Zhang, Y.; Li, P.F.; Liao, W.Q.; Xiong, R.G. A Three-Dimensional Lead Halide Perovskite-Related Ferroelectric. *J. Am. Chem. Soc.* **2020**, *142*, 4604–4608. [[CrossRef](#)]
7. Saparov, B.; Mitzi, D.B. Organic-Inorganic Perovskites: Structural Versatility for Functional Materials Design. *Chem. Rev.* **2016**, *116*, 4558–4596. [[CrossRef](#)]
8. Travis, W.; Glover, E.N.K.; Bronstein, H.; Scanlon, D.O.; Palgrave, R.G. On the application of the tolerance factor to inorganic and hybrid halide perovskites: A revised system. *Chem. Sci.* **2016**, *7*, 4548–4556. [[CrossRef](#)]
9. Ramos-Terrón, S.; Jodlowski, A.D.; Verdugo-Escamilla, C.; Camacho, L.; De Miguel, G. Relaxing the Goldschmidt Tolerance Factor: Sizable Incorporation of the Guanidinium Cation into a Two-Dimensional Ruddlesden-Popper Perovskite. *Chem. Mater.* **2020**, *32*, 4024–4037. [[CrossRef](#)]
10. Grancini, G.; Nazeeruddin, M.K. Dimensional tailoring of hybrid perovskites for photovoltaics. *Nat. Rev. Mater.* **2019**, *4*, 4–22. [[CrossRef](#)]
11. Lyu, R.; Moore, C.E.; Liu, T.; Yu, Y.; Wu, Y. Predictive Design Model for Low-Dimensional Organic-Inorganic Halide Perovskites Assisted by Machine Learning. *J. Am. Chem. Soc.* **2021**, *143*, 12766–12776. [[CrossRef](#)] [[PubMed](#)]
12. Xu, F.; Li, Y.; Liu, N.; Han, Y.; Zou, M.; Song, T. 1D perovskitoid as absorbing material for stable solar cells. *Crystals* **2021**, *11*, 241. [[CrossRef](#)]
13. Wang, J.; Liu, L.; Chen, S.; Qi, L.; Zhao, M.; Zhao, C.; Tang, J.; Cai, X.; Lu, F.; Jiu, T. Growth of 1D Nanorod Perovskite for Surface Passivation in FAPbI₃ Perovskite Solar Cells. *Small* **2022**, *18*, 1–9. [[CrossRef](#)]
14. Marchenko, E.I.; Korolev, V.V.; Mitrofanov, A.; Fateev, S.A.; Goodilin, E.A.; Tarasov, A.B. Layer Shift Factor in Layered Hybrid Perovskites: Univocal Quantitative Descriptor of Composition-Structure-Property Relationships. *Chem. Mater.* **2021**, *33*, 1213–1217. [[CrossRef](#)]
15. Marchenko, E.I.; Korolev, V.V.; Fateev, S.A.; Mitrofanov, A.; Eremin, N.N.; Goodilin, E.A.; Tarasov, A.B. Relationships between Distortions of Inorganic Framework and Band Gap of Layered Hybrid Halide Perovskites. *Chem. Mater.* **2021**, *33*, 7518–7526. [[CrossRef](#)]
16. Wong, W.P.D.; Hanna, J.V.; Grimsdale, A.C. The classification of 1D ‘perovskites’. *Acta Crystallogr. Sect. B Struct. Sci. Cryst. Eng. Mater.* **2021**, *77*, 307–308. [[CrossRef](#)]
17. Blatov, V.A.; Shevchenko, A.P.; Proserpio, D.M. Applied topological analysis of crystal structures with the program package topospro. *Cryst. Growth Des.* **2014**, *14*, 3576–3586. [[CrossRef](#)]
18. Blatov, V.A.; Proserpio, D.M. Topological relations between three-periodic nets. II. Binodal nets. *Acta Crystallogr. A.* **2009**, *65*, 202–212. [[CrossRef](#)]
19. Groom, C.R.; Bruno, I.J.; Lightfoot, M.P.; Ward, S.C. The Cambridge structural database. *Acta Crystallogr. Sect. B Struct. Sci. Cryst. Eng. Mater.* **2016**, *72*, 171–179. [[CrossRef](#)]
20. Blatov, V.A.; O’Keeffe, M.; Proserpio, D.M. Vertex-, face-, point-, Schläfli-, and Delaney-symbols in nets, polyhedra and tilings: Recommended terminology. *CrystEngComm* **2010**, *12*, 44–48. [[CrossRef](#)]
21. Giannozzi, P.; Baroni, S.; Bonini, N.; Calandra, M.; Car, R.; Cavazzoni, C.; Ceresoli, D.; Chiarotti, G.L.; Cococcioni, M.; Dabo, I.; et al. QUANTUM ESPRESSO: A modular and open-source software project for quantum simulations of materials. *J. Phys. Condens. Matter* **2009**, *21*, 395502. [[CrossRef](#)] [[PubMed](#)]
22. Giannozzi, P.; Barone, G.; Bonfà, P.; Brunato, D.; Car, R.; Carnimeo, I.; Cavazzoni, C.; De Gironcoli, S.; Delugas, P.; Ferrarri Ruffino, F.; et al. Quantum ESPRESSO toward the exascale. *J. Chem. Phys.* **2020**, *152*, 154105. [[CrossRef](#)] [[PubMed](#)]
23. Nishihara, S. Burai 1.3, A GUI of Quantum ESPRESSO. Available online: <https://burai.readthedocs.io/en/latest/> (accessed on 27 March 2022).
24. Perdew, J.P.; Burke, K.; Ernzerhof, M. Generalized Gradient Approximation Made Simple. *Phys. Rev. Lett.* **1996**, *77*, 3865–3868. [[CrossRef](#)] [[PubMed](#)]
25. Lin, J.S.; Qteish, A.; Payne, M.C.; Heine, V. Optimized and transferable nonlocal separable ab initio pseudopotentials. *Phys. Rev. B* **1993**, *47*, 4174–4180. [[CrossRef](#)]
26. Momma, K.; Izumi, F. VESTA 3 for three-dimensional visualization of crystal, volumetric and morphology data. *J. Appl. Crystallogr.* **2011**, *44*, 1272–1276. [[CrossRef](#)]
27. Fateev, S.A.; Petrov, A.A.; Marchenko, E.I.; Zubavichus, Y.V.; Khrustalev, V.N.; Petrov, A.V.; Aksenov, S.M.; Goodilin, E.A.; Tarasov, A.B. FA₂PbBr₄: Synthesis, Structure, and Unusual Optical Properties of Two Polymorphs of Formamidinium-Based Layered (110) Hybrid Perovskite. *Chem. Mater.* **2021**, *33*, 1900–1907. [[CrossRef](#)]
28. Mokhnache, O.; Boughzala, H. Crystal structure of a new hybrid compound based on an iodidoplumbate(II) anionic motif. *Acta Crystallogr. Sect. E Crystallogr. Commun.* **2016**, *72*, 56–59. [[CrossRef](#)]
29. Cao, J.; Jing, X.; Yan, J.; Hu, C.; Chen, R.; Yin, J.; Li, J.; Zheng, N. Identifying the Molecular Structures of Intermediates for Optimizing the Fabrication of High-Quality Perovskite Films. *J. Am. Chem. Soc.* **2016**, *138*, 9919–9926. [[CrossRef](#)]
30. Wilke, M.; Casati, N. Insight into the Mechanochemical Synthesis and Structural Evolution of Hybrid Organic-Inorganic Guanidinium Lead(II) Iodides. *Chem. A Eur. J.* **2018**, *24*, 17701–17711. [[CrossRef](#)]

31. Hartono, N.T.P.; Sun, S.; Gélvez-Rueda, M.C.; Pierone, P.J.; Erodici, M.P.; Yoo, J.; Wei, F.; Bawendi, M.; Grozema, F.C.; Sher, M.-J.; et al. The effect of structural dimensionality on carrier mobility in lead-halide perovskites. *J. Mater. Chem. A* **2019**, *7*, 23949–23957. [[CrossRef](#)]
32. Wang, S.; Mitzi, D.B.; Feild, C.A.; Guloy, A. Synthesis and Characterization of $[\text{NH}_2\text{C}(\text{I})\text{:NH}_2]_3\text{MI}_5$ (M = Sn, Pb): Stereochemical Activity in Divalent Tin and Lead Halides Containing Single. *J. Am. Chem. Soc.* **1995**, *117*, 5297–5302. [[CrossRef](#)]
33. Liu, G.-N.; Shi, J.-R.; Han, X.-J.; Zhang, X.; Li, K.; Li, J.; Zhang, T.; Liu, Q.-S.; Zhang, Z.-W.; Li, C. A comparison study of aliphatic and aromatic structure directing agents influencing the crystal and electronic structures, and properties of iodoplumbate hybrids: Water induced structure conversion and visible light photocatalytic properties. *Dalton Trans.* **2015**, *44*, 12561–12575. [[CrossRef](#)] [[PubMed](#)]